Since January 2020 Elsevier has created a COVID-19 resource centre with free information in English and Mandarin on the novel coronavirus COVID-19. The COVID-19 resource centre is hosted on Elsevier Connect, the company's public news and information website.

Journal of Materials Science & Technology 84 (2021) 59–64

Contents lists available at ScienceDirect

Journal of Materials Science & Technology

journal homepage: www.jmst.org

Letter

Cu-bearing high-entropy alloys with excellent antiviral properties

The worldwide outbreak of COVID-19 since December 2019 has caused great challenges to health organizations, and brought tremendous impact on the global economy. There have been over 62.3 million confirmed infection cases and 1.4 million deaths reported until now (December 1 st, 2020), and the numbers are still growing [1]. Although not as influential as COVID-19, the other two large pandemics, severe acute respiratory syndrome (SARS, outbroke in 2002) and Middle East respiratory syndrome (MERS, outbroke in 2012), were also caused by coronaviruses and resulted in severe public health and economic crises in several countries [2,3]. Accompanied by the globalization, the highly connected human society through air travel and conventions offers convenience for the rapid spreading of viruses. Moreover, the occurrence of undetected viruses and their high spontaneous mutation rate challenge the cognitive process and the development of antiviral agents. In this view, the development of broad-spectrum antiviral strategies for prevention and control of viral transmission is of great importance for protecting our human society.

Viruses are obligate parasites that can only replicate inside living cells. Viruses in form of independent particles are called virions, which are composed of at least two parts: (1) genetic material (DNA or RNA) and (2) a protein coat surrounding and protecting the genetic material. Some viruses may also be enveloped in a lipid capsule, when they are released from the host cells. The spreading of viruses varies greatly depending on the specific species, infectivity, and the subsequent relationship with the host. Viruses causing epidemic diseases, e.g., COV-2019, always spread through many routes such as air, water, respiratory droplets, food, and surface contact etc. Much research has focused on the development of antiviral agents that can disrupt the viral replication cycle or destroy them completely [4]. However, the utilization of antiviral materials to block the viral transmission, before they contact human cells, can be meaningful in many applications, such as the healthcare, pharmaceutical manufacturing, food processing, public transport and facilities and scientific research etc.

The utilization of metallic copper (Cu) for antimicrobial applications has attracted for a long-time enormous attention in infection control, including medical implants. The proper addition of Cu in alloys has been confirmed to be biologically safe and efficient in inhibition of many microorganisms non-selectively [5]. Several mechanisms have been proposed to illustrate the intrinsic mechanisms of the copper-mediated antimicrobial function including disruption of cellular membranes resulting from direct contact, reactive hydroxyl radicals generated through Fenton reactions, and ligand interactions mediated by copper ions destroying the structure and integrity of DNA and RNA etc. [6,7]. Since metallic copper can react with multiple active sites without selectivity to the cells, its broad-spectrum antimicrobial efficacy is well known besides the low possibility for pathogens to develop a resistance. Besides the antibacterial and antifungal properties, metallic copper has also been reported for antiviral applications as a constituent in alloys or as a functional additive [8,9].

Cu bearing metals, such as Cu-bearing stainless steels and Cu-bearing titanium alloys, have been widely investigated for their antibacterial properties [10,11]. The increase of copper content, within the limit ranges, has been proven to enhance the antimicrobial activity [12,13]. However, the addition of copper in selective metallic materials might hamper the corrosion resistance and mechanical properties, leading to the non-desirable performance for practical applications [14,15]. Liu et al. illustrated that at least 5% (w/w) of Cu in Ti-Cu alloys was required to obtain a stable antibacterial efficiency [12], but only a 75% reduction of bacterial cell numbers was achieved for Ti-10 Cu alloy (containing 10% Cu) against anaerobic *Porphyromonas gingivalis* over 24 h of incubation [16]. This reduction is insufficient to warrant an industrial application. Recently, the high-entropy alloys (HEAs), accomplished by the combination of multiple principle elements in relatively high concentrations (often in equi-atomic concentrations), have attracted much attention because of their exceptional properties [17]. One interesting approach for manufacturing structural materials with antiviral abilities can be achieved by the fabrication of Cu-bearing HEAs (Cu-HEAs). Owing to the huge design space of HEAs, their antiviral function can lead to a promising future for preparing antiviral materials.

To investigate the feasibility of Cu-HEAs for antiviral applications, the HEA ingots were prepared by vacuum arc melting in a Ti-gettered argon atmosphere. Equal molar ratios of commercially pure Co, Cr, Cu, Ni (99.9%, w/w), and Fe (99.5%–99.6%, w/w) were put into a water-cooled copper crucible. During the arc melting, the ingots were flipped over and remelted for at least five times to ensure the chemical homogeneity. The phase constitution of this CuFeCrCoNi HEA was measured using an X-ray diffractometer (XRD, Empyrean) through scanning 2θ degree from 20° to 100° at a rate of 4°/min. As shown in Fig. 1(a), two disordered face-centered-cubic solid solid-solution phases (FCC1 and FCC2) were observed on the CuFeCrCoNi surfaces. According to the Bragg equation, the lattice constants of the two FCC phases were 3.6138 Å and 3.5820 Å, respectively. The microstructures and micro-area compositions were also analyzed using an electron probe microanalyzer (EPMA, JXA-8530 F PLUS) in back scattered electron (BSE) mode equipped with a wavelength dispersion spectrometer (WDS). The BSE-images are shown in Fig. 1(b) and the chemical compositions of different regions are listed in Table 1. It is clear that the alloy exhibited typical dendrite and interdendrite structures. The WDS results indicated that the gray dendrite regions (illustrated as “A” in Fig. 1(b)) enriched with Co, Cr, Fe and Ni elements, and the four elements uniformly distributed in the alloy. However, the white interdendrite regions (illustrated as “B” in Fig. 1(b)) were mainly composed of the Cu element, accounting for about 80% of the atomic ratio.

https://doi.org/10.1016/j.jmst.2020.12.027

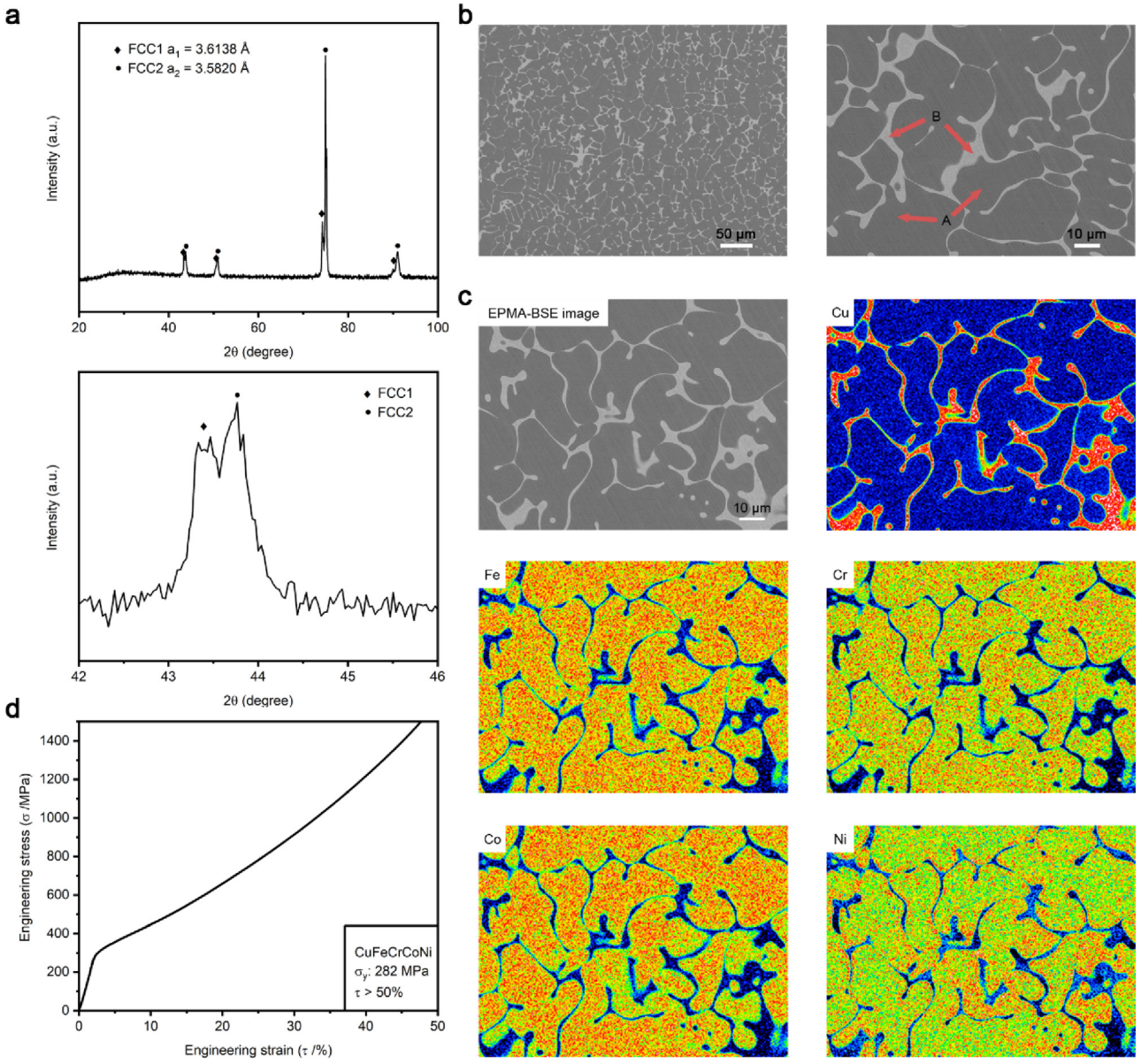

Fig. 1. Characterization of the material properties of the CuFeCrCoNi HEA: (a) XRD analysis, (b) EPMA-BSE images, (c) elemental mapping distribution, and (d) engineering compressive curve. In Fig. 1(b), "A" indicates the dendrite regions and "B" indicates the interdendrite regions. In Fig. 1(c), those images are from the same field of the EPMA-BSE image.

Table 1
Chemical composition (at%) of different regions of the CuFeCrCoNi HEA measured by EPMA-WDS.

Region	Cu	Fe	Cr	Co	Ni
Dendrite region (A)	9.88	23.28	23.00	23.67	20.18
Interdendrite region (B)	84.00	3.21	2.65	3.38	6.76

These results were further corroborated by the elemental mapping distribution, as demonstrated in Fig. 1(c). The compressive property of the CuFeCrCoNi HEA was conducted at room temperature according to the standard of ASTM E9−09 using cylindrical samples of $\phi 5 \times 10$ mm at a compression of 10^{-3} s^{-1}. Fig. 1(d) displays the engineering compression curve showing that the CuFeCrCoNi HEA exhibited excellent plasticity with a compression ratio of over 50% and its yield strength was 282 MPa.

The antiviral properties of the CuFeCrCoNi HEA against influenza virus H1N1 and enterovirus 71 were analyzed by the Guangdong Detection Center of Microbiology (Guangzhou, China) according to the ISO 21702:2019 standard. Coupons with a surface size of 10 mm × 10 mm were cleaned using 70% (v/v) ethanol. Then 0.1 mL virus suspension at approximately 10^6 plaque forming units (PFU) per mL was dipped on the surface. A polyethylene film with a thickness of 0.1 mm was covered on the surface. After 24 h of incubation at 25 °C with a relative humidity no less than 90%, 2 mL maintenance medium was added to recover the viruses. A serial of 10-fold dilutions were prepared and 0.1 mL of each solution was added into the wells containing the host cell monolayers. After incubation at 34 °C in the CO_2 incubator for 1 h, 3 mL of the agar medium was poured into the wells for plaque assay. After 3 d incubation in the CO_2 incubator, formalin solution was used to fix the cells and methylene blue solution was used to dye the cells. If half of the wells were infected by the corresponding viruses, the dilution numbers (D) were recorded. The tissue culture infective doses ($TCID_{50}$) were calculated as 10^D. The antiviral efficacy was calculated as $[(U_0-U_t)-(U_0-U_c)]/U_c$, wherein U_0 means the $TCID_{50}$ of

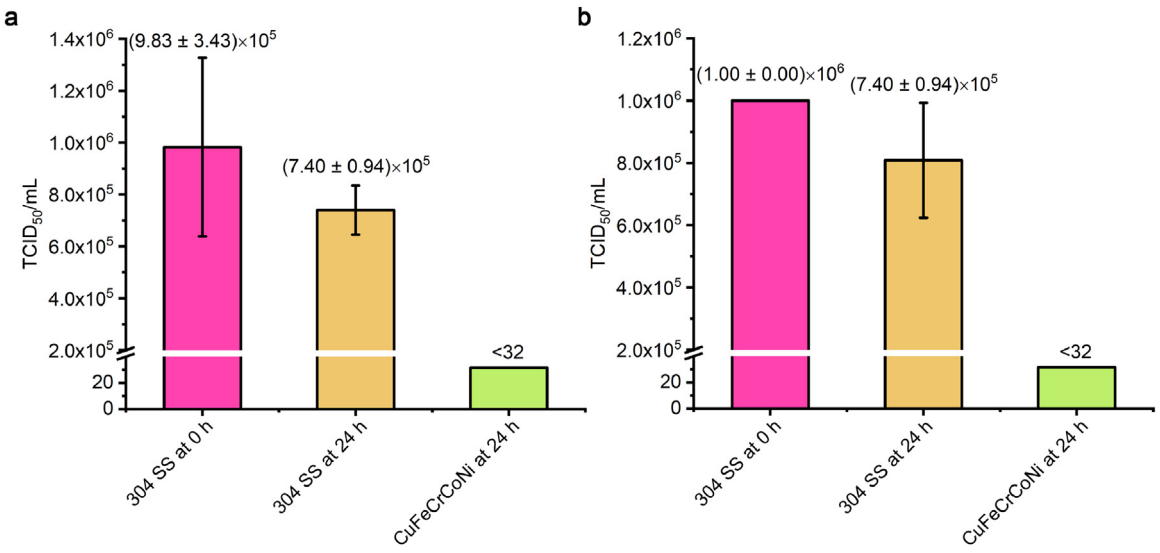

Fig. 2. Antiviral properties of the CuFeCrCoNi HEA against two viruses: (a) influenza virus H1N1 and (b) enterovirus 71. Standard deviations are from at least 3 parallel tests.

the control samples (304 stainless steel) at 0 h, U_t the $TCID_{50}$ of the treated samples at 24 h, and U_c the $TCID_{50}$ of control samples at 24 h.

As shown in Fig. 2, after 24 h incubation on 304 SS coupons, over 70% of H1N1 viruses were still alive, and were still able to infect Madin-Darby canine kidney (MDCK) cells. However, more than 99.99% of the H1N1 viruses on the CuFeCrCoNi HEA had been inactivated after 24 h of incubation (Fig. 2(a)). Also, over 99.99% of the enterovirus 71 viruses had been inactivated, whereas over 93.3% of the viruses on 304 SS surfaces were still able to infect Vero cells after 24 h (Fig. 2(b)). These results indicate that CuFeCrCoNi HEA is capable of efficient inactivation of these virus types.

The addition of element aluminum into HEAs has been verified to induce the formation of new phases and then to precipitate out in the HEAs, which increases the mechanical strengths of HEAs [18,19]. Various research has focused on the effect of the aluminum content on the microstructure and properties of different HEAs, including Al_xCoCrCuFeNi [20,21], Al_xCoCrFeNi [22], and TiC reinforced Al_xFeCoNiCu [23] and so on. A gradual change from single FCC phase to duplex FCC-BCC phase, then to single BCC phase, was observed with an increase of aluminum content. The formation of BCC phase in the FCC phase increases the strength. However, it hampers the ductility, which leads to brittleness at ambient temperature [24]. Consequently, the addition of aluminum at an appropriate content is necessary to achieve excellent properties. Moreover, because of its low mass density, the addition of aluminum is an effective way to reduce the HEA density. Herein, we tested further the corrosion and antiviral properties of $Al_{0.4}$CoCrCuFeNi HEA [25], which also possesses both FCC1 and FCC2 phases, to illustrate the influence of aluminum addition on the properties of Cu-HEAs and to pave the way for further pursuing antiviral HEAs with remarkable performance.

In Fig. 3, data from electrochemical analyses are presented to analyze the influence of aluminum addition on the corrosion properties of Cu-HEAs. The polarization resistance (R_p) of the Cu-HEAs increased from 28.8 ± 7.9 kΩ cm^2 for the CuFeCrCoNi HEA to 358.3 ± 25.7 kΩ cm^2 for the $Al_{0.4}$CuFeCrCoNi HEA (Fig. 3(a)) in 3.5% NaCl. This suggests significant increase in corrosion resistance. An R_p value of 27.0 ± 6.3 kΩ cm^2 was measured for 304 stainless steel (304SS), which is similar to the CuFeCrCoNi HEA and far below that of the $Al_{0.4}$CuFeCrCoNi HEA (Fig. 3(a)). The corrosion parameters, including corrosion potential (E_{corr}) and corrosion current density (i_{corr}), were calculated through the Tafel curve fitting of the cyclic polarization curves in Fig. 3(b). The open current potential (E_{OCP}) and E_{corr} were almost the same for the two Cu-HEAs (Table 2). However, the i_{corr} decreased from 780 ± 212 nA cm^{-2} for the CuFeCrCoNi HEA, which was similar with the value for 304SS, to 213 ± 101 nA cm^{-2} for the $Al_{0.4}$CuFeCrCoNi HEA (Fig. 3(a)). This confirms further the decrease of corrosion tendency of CuFeCrCoNi HEA due to an aluminum addition. Moreover, with the addition of Al, the passivation behavior was observed on the polarization curve of $Al_{0.4}$CuFeCrCoNi HEA, which did not occur with the CuFeCrCoNi HEA. The breakdown potential of the $Al_{0.4}$CuFeCrCoNi HEA was lower than that of 304SS, indicating a better pitting corrosion resistance of 304 SS.

Table 2
Electrochemical parameters of the two Cu-HEAs.

	E_{OCP} (mV) vs. SCE	E_{corr} (mV) vs. SCE
304SS	−258.3 ± 35.1	−285.7 ± 42.7
CuFeCrCoNi	−195.4 ± 47.7	−228.6 ± 23.1
$Al_{0.4}$CuFeCrCoNi	−196.5 ± 28.3	−232.0 ± 18.5

The antiviral properties of the $Al_{0.4}$CuFeCrCoNi HEA against the influenza virus H1N1 and the enterovirus 71 were also tested. As shown in Fig. 4(a), after 24 h of treatment, over 99.99% of H1N1 viruses have been inactivated on $Al_{0.4}$CuFeCrCoNi HEA surfaces and were non-infectious anymore. Also, an antiviral effect of over 99.99% was obtained for the $Al_{0.4}$CuFeCrCoNi HEA against enterovirus 71 (Fig. 4(b)). The $Al_{0.4}$CuFeCrCoNi HEA displayed a similar antiviral activity as compared with the CuFeCrCoNi HEA. Obviously, the addition of Al with proper content did not influence antiviral efficiency of the Cu-HEAs.

HEAs are currently in the focus of interesting metallurgy because of many possible innovative applications in various industries. One main reason of the use of HEAs distinctive from conventional materials are the outstanding mechanical properties. The most noticeable examples are the FCC CrCoNi-based alloys [26,27]. Here, the CuFeCrCoNi HEA was made through adding the two metals Fe and Cu into the CrCoNi-based alloy. In the product only FCC phases were observed by XRD analysis. The excellent yield stress values of these Cu-HEAs (282 MPa for the CuFeCrCoNi HEA and 318 MPa for the $Al_{0.4}$CuFeCrCoNi HEA [25]), which by far exceed those of 304 Cu-SS (185 MPa [25]) and 316 L/317 L N Cu-SS (~230 MPa [28,29]), are a result of the specific interactions among the various metal atoms in these HEAs. Consequently, such materials can meet the performance requirements for vari-

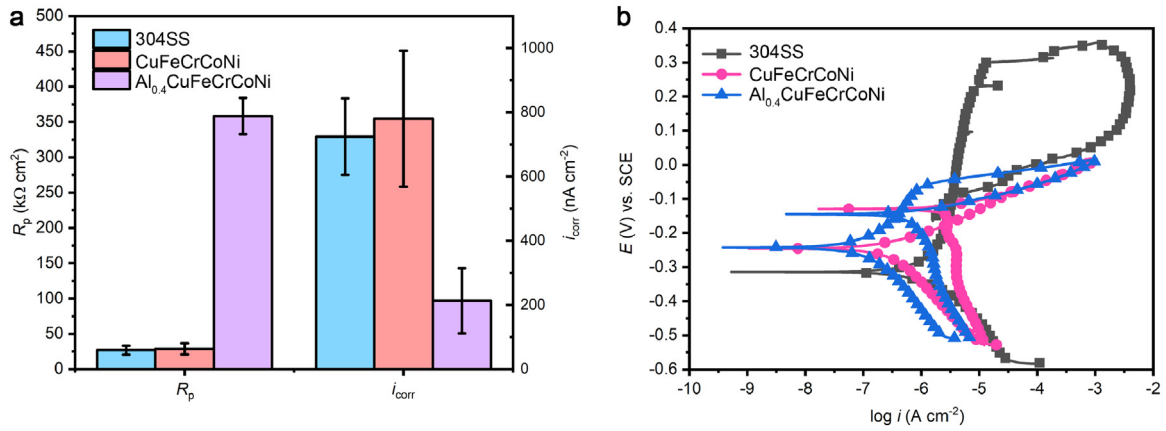

Fig. 3. Electrochemical analysis of the corrosion resistance of two Cu-HEAs: (a) R_p and i_{corr} and (b) polarization curves. Standard deviations are from at least 3 parallel tests.

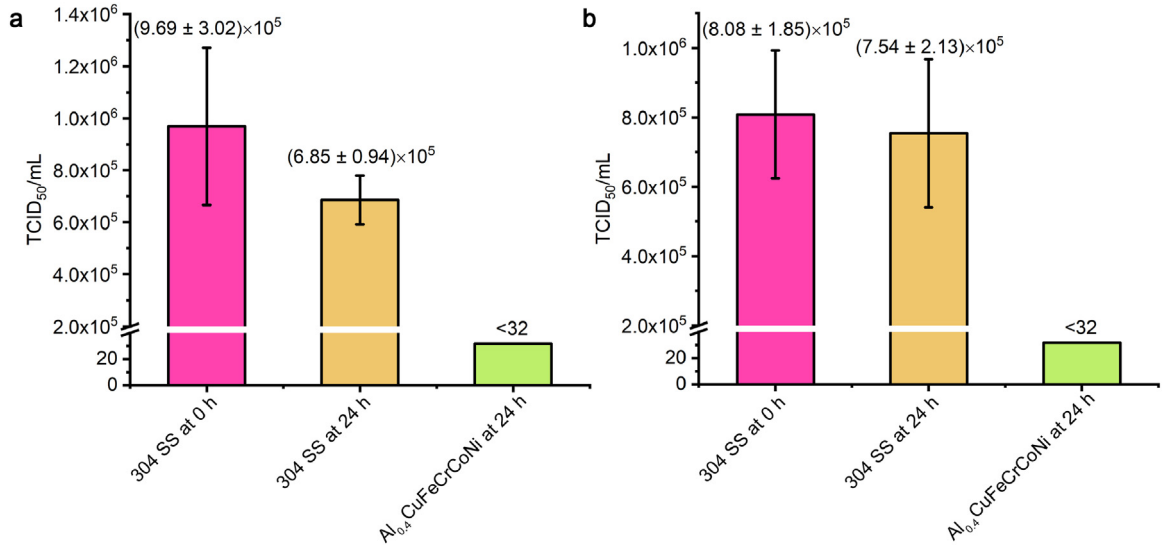

Fig. 4. Antiviral properties of the $Al_{0.4}CuFeCrCoNi$ HEA against two viruses: (a) influenza virus H1N1 and (b) enterovirus 71. Standard deviations are from at least 3 parallel tests.

ous special applications. Besides excellent mechanical properties, the next generation of HEAs should focus on novel materials with unprecedented properties [30,31]. In this study, excellent antiviral properties were observed through the incorporation of copper into HEA. Cu accounts for approximately 20 at.% in the Cu-HEAs, which far exceed that of classical antimicrobial metals such as antibacterial stainless steels and antibacterial titanium alloys. Previously, the $Al_{0.4}CuFeCrCoNi$ HEA had demonstrated its broad-spectrum antibacterial performance [25]. In view of this, the addition of other antimicrobial metals, such as argentum (Ag) and zinc (Zn), might be used also for the development of antiviral HEAs.

Depending on various antiviral mechanisms, numerous antiviral materials have been developed, such as metallic nanoparticles, carbon-based nanomaterials, organic nanomaterials, and antiviral biopolymers which were synthesized either artificially or extracted from natural resources [32,33]. Such functional nanomaterials are restricted always by high cost due to the complicated manufacturing process. In addition, though much attention has been paid to their unique physicochemical characteristics, nanomaterials are still questionable considering their potential toxicity toward humans and their environmental risks [33,34]. The large specific surface area of nanomaterials enables them to interact closely with intracellular substances, e.g. nucleic acids, proteins and enzymes, which might cause yet unknown detrimental effects on cells and tissues [35]. Biopolymers, mostly isolated from natural resources, are promising candidates for antiviral applications. Some polysaccharides [36], poly- and oligonucleotides [37], peptides [38], and proteins [39] have been confirmed to possess broad-spectrum antiviral activities and low adverse effects. However, because of their low mechanical strength and low product yields, those antiviral biopolymers can only be utilized in highly specialized areas, such as biomedical applications and fabrication of protective appliances. Copper alloys have long been recognized for their antiviral properties against various viruses including herpes simplex virus [40], noroviruses [41], and influenza virus [42]. Several mechanisms have been proposed to elucidate the inactivation of viruses by metallic copper. The released copper ions (i.e., Cu^+ and Cu^{2+}) during aqueous corrosion might chelate with the nucleic acids and the proteins, resulting in the denaturation of virus [40,43]. The oxidative agents produced during the electrochemical corrosion processes can also participate and accelerate the inactivation processes [40,44]. On the other hand, the direct contact of solid metallic oxides, especially Cu_2O, formed on the alloy surfaces can also lead to the denaturation of structural proteins, which results in the inactivation of viruses [42]. Engineered Cu-HEAs offer a viable strategy for usable antiviral structural materials, which can be applied in food manufacturing, public transportation, medical instruments, therapeutic appliance, and public sanitary places etc.

In conclusion, we propose a novel concept for the design of antiviral metallic materials. The addition of copper into HEAs

endows the materials with excellent antiviral properties. Further optimization of alloying compositions, e.g. an aluminum addition, can neutralize the drawbacks caused by copper addition. Furthermore, we illustrate two Cu-HEAs with efficient antiviral properties. Over 99.99% of influenza virus H1N1 and enterovirus 71 were inactivated on the surfaces of such Cu-HEAs and, thus, non-infectious anymore after 24 h of treatment. The design concepts proposed here can guide the design of various types of antiviral Cu-HEAs with excellent mechanical properties and corrosion resistant performance.

Acknowledgements

This research was financially supported by the Fundamental Research Funds for the Central Universities (Nos. N2002020 and N2002019), the National Natural Science Foundation of China (Nos. 51871050, 5184022, and 51901039), the National Key Research and Development Program of China (Nos. 2019YFA0209901 and 2018YFA0702901), the fund of the State Key Laboratory of Solidification Processing in NWPU (No. SKLSP201902), and the Fund of Science and Technology on Reactor Fuel and Materials Laboratory (STRFML-2020-04).

References

[1] WHO, Coronavirus Disease (COVID-19) Dashboard, 2020 https://covid19.who.int/.
[2] R.M. Anderson, C. Fraser, A.C. Ghani, C.A. Donnelly, S. Riley, N.M. Ferguson, G.M. Leung, T.H. Lam, A.J. Hedley, Philos. Trans. R. Soc. Lond. B-Biol. Sci. 359 (2004) 1091–1105.
[3] F.S. Alhamlan, M.S. Majumder, J.S. Brownstein, J. Hawkins, H.M. Al-Abdely, A. Alzahrani, D.A. Obaid, M.N. Al-Ahdal, A. BinSaeed,BMJ Open 7 (2017), e011865.
[4] E. Paintsil, Y.C. Cheng, in: T.M. Schmidt (Ed.), Encyclopedia of Microbiology, 4th edn, Academic Press, 2019, pp.176-225.65.
[5] E.L. Zhang, S. Fu, R.X. Wang, H.X. Li, Y. Liu, Z.Q. Ma, G.K. Liu, C.S. Zhu, G.W. Qin, D.F. Chen, Rare Met. 38 (2019) 476–494.
[6] G. Grass, C. Rensing, M. Solioz, Appl. Environ. Microbiol. 77 (2011) 1541–1547.
[7] M. Vincent, R.E. Duval, P. Hartemann, M. Engels-Deutsch, J. Appl. Microbiol. 124 (2018) 1032–1046.
[8] T.M. Gross, J. Lahiri, A. Golas, J. Luo, F. Verrier, J.L. Kurzejewski, D.E. Baker, J. Wang, P.F. Novak, M.J. Snyder, Nat. Commun. 10 (2019) 1979.
[9] S.L. Warnes, E.N. Summersgill, C.W. Keevil, Appl. Environ. Microbiol. 81 (2015) 1085–1091.
[10] X. Zhang, C. Yang, K. Yang, ACS Appl. Mater. Interfaces 12 (2020) 361–372.
[11] M. Li, Z. Ma, Y. Zhu, H. Xia, M. Yao, X. Chu, X. Wang, K. Yang, M. Yang, Y. Zhang, C. Mao, Adv. Healthc. Mater. 5 (2016) 557–566.
[12] J. Liu, F. Li, C. Liu, H. Wang, B. Ren, K. Yang, E. Zhang, Mater. Sci. Eng. C 35 (2014) 392–400.
[13] E. Zhang, J. Ren, S. Li, L. Yang, G. Qin,Biomed. Mater. 11 (2016), 065001.
[14] S. Chen, X. Dong, R. Ma, L. Zhang, H. Wang, Z. Fan, Mater. Sci. Eng. A 551 (2012) 87–94.
[15] S.Q. Chen, X.P. Dong, X.Q. Xiong, R. Ma, Z.T. Fan, Adv. Mater. Res. 463−464 (2012) 52–57.
[16] B. Bai, E. Zhang, J. Liu, J. Zhu, Dent. Mater. J. 35 (2016) 659–667.
[17] E.P. George, D. Raabe, R.O. Ritchie, Nat. Rev. Mater. 4 (2019) 515–534.
[18] M.H. Chuang, M.H. Tsai, W.R. Wang, S.J. Lin, J.W. Yeh, Acta Mater. 59 (2011) 6308–6317.
[19] S.T. Chen, W.Y. Tang, Y.F. Kuo, S.Y. Chen, C.H. Tsau, T.T. Shun, J.W. Yeh, Mater. Sci. Eng. A 527 (2010) 5818–5825.
[20] J.M. Wu, S.J. Lin, J.W. Yeh, S.K. Chen, Y.S. Huang, H.C. Chen, Wear 261 (2006) 513–519.
[21] C.J. Tong, Y.L. Chen, S.K. Chen, J.W. Yeh, T.T. Shun, C.H. Tsau, S.J. Lin, S.Y. Chang, Metall. Mater. Trans. A 36 (2005) 881–893.
[22] W.R. Wang, W.L. Wang, S.C. Wang, Y.C. Tsai, C.H. Lai, J.W. Yeh, Intermetallics 26 (2012) 44–51.
[23] X. Sun, H. Zhu, J. Li, J. Huang, Z. Xie, Mater. Sci. Eng. A 743 (2019) 540–545.
[24] W.J. Kim, H.T. Jeong, H.K. Park, K. Park, T.W. Na, E. Choi, J. Alloy. Compd. 802 (2019) 152–165.
[25] E. Zhou, D. Qiao, Y. Yang, D. Xu, Y. Lu, J. Wang, J.A. Smith, H. Li, H. Zhao, P.K. Liaw, F. Wang, J. Mater. Sci. Technol. 46 (2020) 201–210.
[26] C.E. Slone, J. Miao, E.P. George, M.J. Mills, Acta Mater. 165 (2019) 496–507.
[27] M. Yang, D. Yan, F. Yuan, P. Jiang, E. Ma, X. Wu, Proc. Natl. Acad. Sci. U.S.A. 115 (2018) 7224–7229.
[28] T. Xi, M.B. Shahzad, D. Xu, Z. Sun, J. Zhao, C. Yang, M. Qi, K. Yang, Mater. Sci. Eng. C 71 (2017) 1079–1085.
[29] T. Xi, C. Yang, M. Babar Shahzad, K. Yang, Mater. Des. 87 (2015) 303–312.
[30] E. Ma, X. Wu, Nat. Commun. 10 (2019) 5623.
[31] Q. Wang, A. Sarkar, D. Wang, L. Velasco, R. Azmi, S.S. Bhattacharya, T. Bergfeldt, A. Düvel, P. Heitjans, T. Brezesinski, H. Hahn, B. Breitung, Energ. Environ. Sci. 12 (2019) 2433–2442.
[32] J. Zhou, Z. Hu, F. Zabihi, Z. Chen, M. Zhu, Adv. Fiber Mater. 2 (2020) 123–139.
[33] L. Liang, A. Ahamed, L. Ge, X. Fu, G. Lisak, ChemPlusChem 85 (2020) 2105–2128.
[34] R. Nho,Nanomedicine 29 (2020), 102242.
[35] J. Zhao, V. Castranova, J. Toxicol. Environ. Health B 14 (2011) 593–632.
[36] W. Wang, S.X. Wang, H.S. Guan, Mar. Drugs 10 (2012) 2795–2816.
[37] A. Vaillant, Antiviral Res. 133 (2016) 32–40.
[38] D.C. Brice, G. Diamond, Curr. Med. Chem. 27 (2020) 1420–1443.
[39] E. Braun, D. Hotter, L. Koepke, F. Zech, R. Gross, K.M.J. Sparrer, J.A. Muller, C.K. Pfaller, E. Heusinger, R. Wombacher, K. Sutter, U. Dittmer, M. Winkler, G. Simmons, M.R. Jakobsen, K.K. Conzelmann, S. Pohlmann, J. Munch, O.T. Fackler, F. Kirchhoff, D. Sauter, Cell Rep. 27 (2019) 2092–2104, e2010.
[40] J.-L. Sagripanti, L.B. Routson, A.C. Bonifacino, C.D. Lytle, Antimicrob. Agents Ch. 41 (1997) 812–817.
[41] S.L. Warnes, C.W. Keevil,PLoS One 8 (2013), e75017.
[42] M. Minoshima, Y. Lu, T. Kimura, R. Nakano, H. Ishiguro, Y. Kubota, K. Hashimoto, K. Sunada, J. Hazard. Mater. 312 (2016) 1–7.
[43] H. Michels, S. Wilks, J. Noyce, C. Keevil, Stainless Steel 77000 (2005) 27.
[44] J.R. Scully, The COVID-19 Pandemic, Part 1: Can Antimicrobial Copper-based Alloys Help Suppress Infectious Transmission of Viruses Originating From Human Contact With High-touch Surfaces? NACE International, 2020.

Zhong Li [a,b]
[a] *Shenyang National Laboratory for Materials Science, Northeastern University, Shenyang, 110819, China*
[b] *Key Laboratory for Anisotropy and Texture of Materials (Ministry of Education), School of Materials Science and Engineering, Northeastern University, Shenyang, 110819, China*

Dongxu Qiao
Key Laboratory of Solidification Control and Digital Preparation Technology (Liaoning Province), School of Materials Science and Engineering, Dalian University of Technology, Dalian, 116024, China

Yan Xu [a,b]
Enze Zhou [a,b]
Chuntian Yang [a,b]
Xinyi Yuan [a,b]
[a] *Shenyang National Laboratory for Materials Science, Northeastern University, Shenyang, 110819, China*
[b] *Key Laboratory for Anisotropy and Texture of Materials (Ministry of Education), School of Materials Science and Engineering, Northeastern University, Shenyang, 110819, China*

Yiping Lu [**]
Key Laboratory of Solidification Control and Digital Preparation Technology (Liaoning Province), School of Materials Science and Engineering, Dalian University of Technology, Dalian, 116024, China

Ji-Dong Gu
Environmental Engineering, Guangdong Technion Israel Institute of Technology, Shantou 515063, China

Sand Wolfgang
Textile Pollution Controlling Engineering Center of Ministry of Environmental Protection, College of Environmental Science and Engineering, Donghua University, Shanghai, 201620, China

Dake Xu [a,b,*]
Fuhui Wang [a,b]
[a] *Shenyang National Laboratory for Materials Science, Northeastern University, Shenyang, 110819, China*
[b] *Key Laboratory for Anisotropy and Texture of Materials (Ministry of Education), School of Materials Science and Engineering, Northeastern University, Shenyang, 110819, China*

** Corresponding author.

* Corresponding author at: Shenyang National Laboratory for Materials Science, Northeastern University, Shenyang, 110819, China.

E-mail addresses: luyiping@dlut.edu.cn (Y. Lu), xudake@mail.neu.edu.cn (D. Xu).

7 December 2020
Available online 27 January 2021